Wear 298–299 (2013) 120–126

Contents lists available at SciVerse ScienceDirect

Wear

journal homepage: www.elsevier.com/locate/wear

Abrasive wear response of nanocrystalline Ni–W alloys across the Hall–Petch breakdown

Timothy J. Rupert [a,b,*], Wenjun Cai [a], Christopher A. Schuh [a]

[a] Department of Materials Science and Engineering, Massachusetts Institute of Technology, 77 Massachusetts Avenue, Cambridge, MA 02139, USA
[b] Department of Mechanical and Aerospace Engineering, University of California, 4200 Engineering Gateway, Irvine, CA 92697, USA

ARTICLE INFO

Article history:
Received 13 August 2012
Received in revised form
1 November 2012
Accepted 10 January 2013
Available online 20 January 2013

Keywords:
Wear testing
Two-body abrasion
Hardness
Electron microscopy
Non-ferrous metals
Nanocrystalline metals

ABSTRACT

The abrasive wear of nanocrystalline Ni–W alloys with grain sizes of 5–105 nm has been studied using Taber abrasion testing. The wear resistance of the finest grain size specimen is found to be higher than would be predicted based on hardness alone. This deviation from Archard scaling is traced to mechanically-driven structural evolution, consisting of grain growth and grain boundary relaxation, which occurs during wear. Comparison of these observations with previous wear studies suggests that the extent of structural evolution during wear depends on contact stresses and material removal rates.
© 2013 Elsevier B.V. All rights reserved.

1. Introduction

Nanocrystalline metals, polycrystals with grain sizes less than 100 nm, are typically very hard and are commonly produced as films, making them promising as coatings which can help mitigate wear-related failures. This promise of improved wear resistance comes from the Archard model that connects wear rate directly to hardness [1].

$$\frac{\partial V}{\partial l} = K \times \frac{P}{H} \tag{1}$$

where V is the volume of worn material, l is the sliding distance, K is called the wear coefficient, P is the applied load, and H is hardness. Wear is an intricate process involving frictional sliding, a time-dependent multi-axial stress state, mechanochemistry, and highly localized plastic deformation. While more complex predictive models have been proposed (e.g., [2]), the Archard model captures the key physics of wear loss (material removal through abrasion or adhesion at asperity contacts) and has been found to accurately predict the wear response of a wide range of engineering metals [3].

Early reports of wear in nanocrystalline metallic systems have supported the notion that these materials are significantly more wear resistant than their microcrystalline counterparts. The majority of prior work has focused on a simple comparison between the wear behavior of microcrystalline metals and a single nanocrystalline grain size [4–9], although limited studies which access multiple nanocrystalline grain sizes do exist in the literature. Farhat et al. [10] explored nanocrystalline Al with pin-on-disk testing, Jeong et al. [11,12] studied nanocrystalline Ni and Ni–P with Taber abrasion testing, and Schuh et al. [13] studied nanocrystalline Ni using nanoscratch experiments. In all three cases, the authors found that the nanocrystalline metals they studied adhered to the Archard equation given in Eq. (1) over a wide range of grain sizes. However, limited data is available for nanocrystalline grain sizes below ~20 nm, where the traditional Hall–Petch relationship connecting strength to grain size breaks down and where grain boundary-dominated deformation physics begin to control the mechanical behavior of nanocrystalline materials. At these finest grain sizes, traditional dislocation tangling and storage give way to more collective mechanisms such as grain boundary sliding and grain rotation [14–16].

Rupert and Schuh [17] recently provided a systematic examination of wear in nanocrystalline metals across the entire Hall–Petch breakdown, reporting deviations from Archard-like scaling for electrodeposited Ni–W alloys with grain sizes below ~15 nm that were subjected to pin-on-disk sliding wear. The finest nanocrystalline grain sizes were found to wear considerably less than would be expected based on their as-deposited hardness. Surface plasticity induced during pin-on-disk experiments caused a modest amount of grain growth and grain boundary relaxation in a distinct, locally-hardened surface layer with a thickness of a few hundred nanometers. By connecting this hardened surface

* Corresponding author at: Department of Mechanical and Aerospace Engineering, University of California, 4200 Engineering Gateway, Irvine, CA 92697, USA.
Tel.: +1 949 824 4937; fax: +1 949 824 8585.
E-mail address: trupert@uci.edu (T.J. Rupert).

0043-1648/$ - see front matter © 2013 Elsevier B.V. All rights reserved.
http://dx.doi.org/10.1016/j.wear.2013.01.021

layer to significant improvements in wear resistance, Rupert and Schuh showed that microstructural evolution can be beneficial for nanocrystalline wear performance under sliding wear conditions.

In the present study, we revisit the nanocrystalline Ni–W system, again addressing wear response across the Hall–Petch breakdown, but using a different wear testing metholodogy: Taber abrasion. Taber abrasion exposes a material to very different conditions than pin-on-disk sliding; low contact stress and fast material removal through particle cutting are characteristic of Taber abrasion. Our goal is to understand if structural evolution and deviations from Archard scaling are general features of nanocrystalline wear or a strong function of testing conditions.

2. Materials and methods

To access a wide range of nanocrystalline grain sizes, Ni–W alloys were created using the pulsed electrodeposition technique and bath chemistry of Detor and Schuh [18,19]. Square carbon steel substrates of 10 cm width were prepared for electrodeposition by pickling with hydrochloric acid and electrocleaning following ASTM Standard B183-79 [20]. Grain size was varied by tuning the applied current waveform and deposition temperature [18], and the deposited coatings were 15–20 μm thick.

The composition of each specimen was determined using energy dispersive spectroscopy (EDS) in a Leo 438VP scanning electron microscope. X-ray diffraction (XRD) profiles were then obtained using a PANalytical X'Pert Pro diffractometer, to ensure that all specimens were polycrystalline fcc solid solutions. The average grain sizes were measured with transmission electron microscopy (TEM) in bright field imaging mode. Each grain was manually identified and traced, and then the equivalent circular diameter was calculated. Cross-sectional TEM specimens were prepared using the focused ion beam (FIB) in situ lift-out technique [21] and examined in a JEOL 2010 operated at 200 kV.

Vickers microhardness of each specimen was measured with a LECO Model LM247 indenter with an applied load of 10 g and a 15 s hold time. Abrasive wear loss was measured with a Taber Rotary Platform Abrasion Tester Model 5135 following ASTM Standard G195-08 [22]. Taber wear testing involves two abrasive wheels placed on the specimen under a constant load, which then drag across the surface and abrade the coating as the sample is rotated. CS-17 Calibrase Al_2O_3 abrasive wheels were used for this study, and were refaced regularly with 150 grit SiC paper to ensure a consistent contact roughness. Test parameters of 1 kg contact load, 72 rotations per minute and 750 total rotation cycles were used. Wear loss was calculated by measuring sample mass before testing and at regular intervals during wear testing, and then converting these mass loss values to volume loss with a density appropriate for each alloy composition (i.e., accounting for the fact that density increases as *W* content increases). The slope of volume loss as a function of test cycles then gives a value for wear rate which can be used to compare against Eq. (1). At least three specimens were tested for each grain size of interest.

3. Results

3.1. Hardness and wear properties

The measured compositions and as-deposited grain sizes (d_o) of our deposits are presented in Table 1. Specimens with grain sizes of d_o=5–105 nm were produced, with grain size decreasing as *W* content increases. Hardness values for the samples are also presented in Table 1, and summarized as a function of grain size in Fig. 1. Initially, hardness increases with grain refinement from 105 to 18 nm. As grain size reduces below 18 nm, however, a plateau in hardness is observed, signifying a breakdown in Hall–Petch scaling. The trend shown in Fig. 1 is broadly consistent with prior studies of the mechanical properties of nanocrystalline metals, nanocrystalline Ni–W in particular [18,23], and the range of grain sizes studied in the present work spans the transition from dislocation-based mechanisms above about 20 nm to grain boundary-dominated deformation below.

Table 1
Microstructural and mechanical properties of Ni–W electrodeposits.

W content (at%)	Average TEM grain size (nm)	Hardness (GPa)	Wear rate ($mm^3\ cycle^{-1}$)
6.7	105	5.9	4.27×10^{-3}
14.1	18	7.3	3.01×10^{-3}
15.8	8	7.4	2.91×10^{-3}
20.2	5	7.3	2.06×10^{-3}

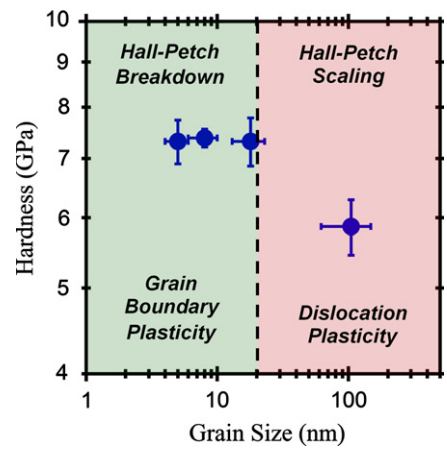

Fig. 1. Hardness of nanocrystalline Ni–W alloys plotted as a function of grain size. (For interpretation of the references to color in this figure, the reader is referred to the web version of this article.)

Fig. 2 shows wear volume loss versus test cycle for all grain sizes and specimens. In general, there is a transient "wear-in" in the first cycles of testing, but for each of our experiments this is apparently concluded within about 250 cycles, after which the data lie on reasonably well-defined lines characterized by a steady-state wear rate. Fig. 3(a) presents the average Taber wear rates of Ni–W specimens plotted against grain size; the trend is essentially monotonic, with wear rate decreasing with grain size. This trend is however not expected on the basis of Archard scaling; if wear rates were in fact inversely proportional to hardness for all of our specimens, the 5 nm specimen would exhibit a wear rate similar to the 8 and 18 nm grain size samples owing to the plateau in hardness seen in Fig. 1. The deviation from Archard scaling can be seen more clearly in Fig. 3(b), where wear rate is plotted against inverse hardness. The Archard equation given in Eq. (1) predicts a linear trend for such a plot (shown in this figure as a dotted blue line) and such proportionality seems reasonably obeyed for the larger grain sizes. Again, however, the finest grain size sample falls well below the Archard prediction, with the 5 nm specimen wearing ~30% less than expected.

3.2. Structural evolution

Previous work from Rupert and Schuh [17] for sliding wear conditions has shown that a deviation from Archard scaling can result from wear-induced structural evolution and an accompanying hardening effect. To investigate the possibility of near-surface microstructural changes under abrasive wear in our specimens,

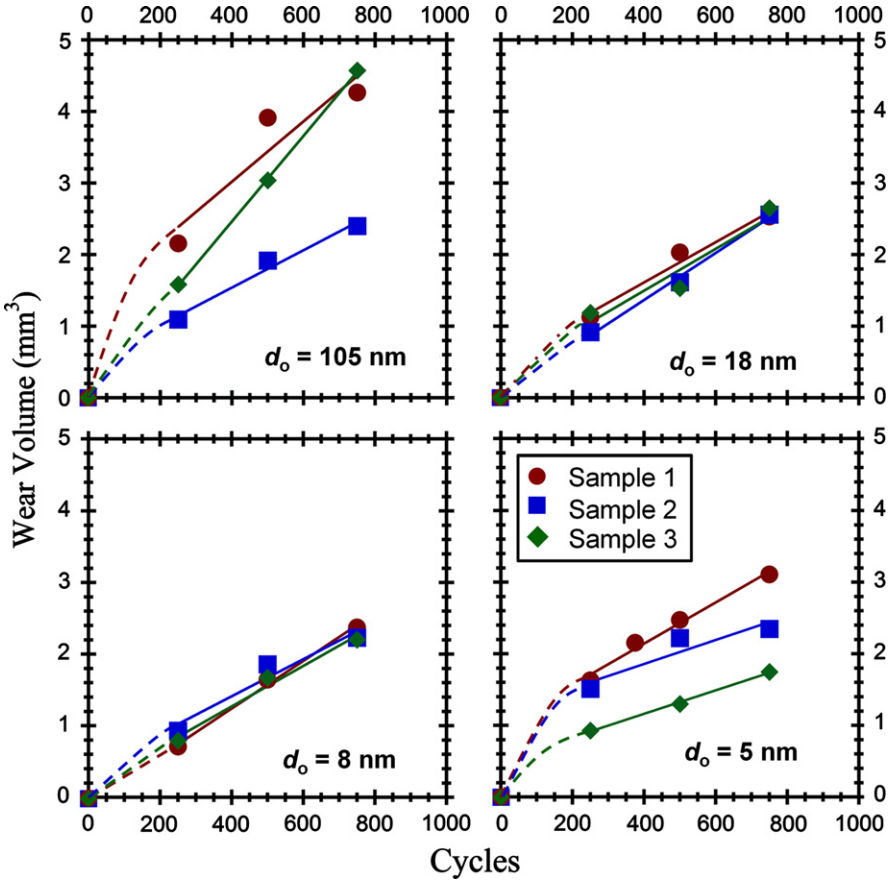

Fig. 2. Wear volume versus test cycle for as-deposited grain sizes of 105 nm, 18 nm, 8 nm, and 5 nm. Some of the curves show a higher apparent wear rate at the outset; this transient "wear-in" regime is denoted by a dashed curve, which transitions to an approximate steady-state regime shown by fitted solid lines.

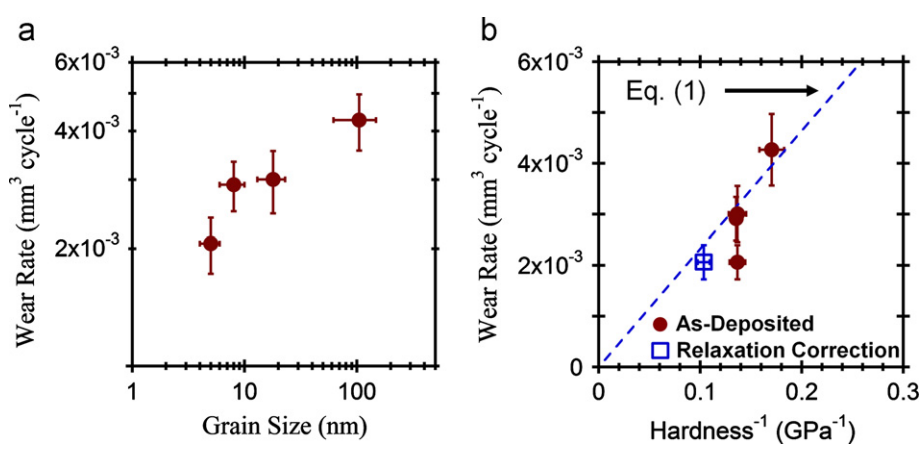

Fig. 3. (a) Wear rate plotted against grain size and (b) wear rate plotted against reciprocal hardness. The Archard equation, which is given in Eq. (1), is shown as a dotted blue line in (b). In (b), the hollow blue point shows where the 5 nm grain size sample would lie if it was corrected for the expected hardening from grain boundary relaxation during wear. (For interpretation of the references to color in this figure legend, the reader is referred to the web version of this article.)

TEM lamellae were cut from the wear surface using the FIB. First, we examine the alloys with larger grain sizes where Archard scaling is followed; bright field cross-sectional TEM micrographs of these samples are presented in Fig. 4. In each image, the wear surface is marked with a dashed white line. Micrographs from our largest grain size, d_o=105 nm, are shown in Fig. 4(a) and (b). Close inspection of Fig. 4(a) shows that some slight grain refinement is observed near the wear surface. Fig. 4(b) presents a magnified view of the near surface region, where a number of grains which are smaller than the as-deposited grain size are observed. Grain refinement is commonly observed in microcrystalline materials as the result of severe plastic deformation at the surface [24,25]. It appears that our largest grain size experiences a similar refinement due to the fact that traditional intragranular dislocation mechanisms still control plastic deformation for grain sizes of ~100 nm and above [14].

Fig. 4(c) and (d) shows the near-surface microstructure in the specimens with d_o=18 and 8 nm, respectively. Comparison of the microstructure near the surface with the material further below shows that the wear process leaves no volume with obvious

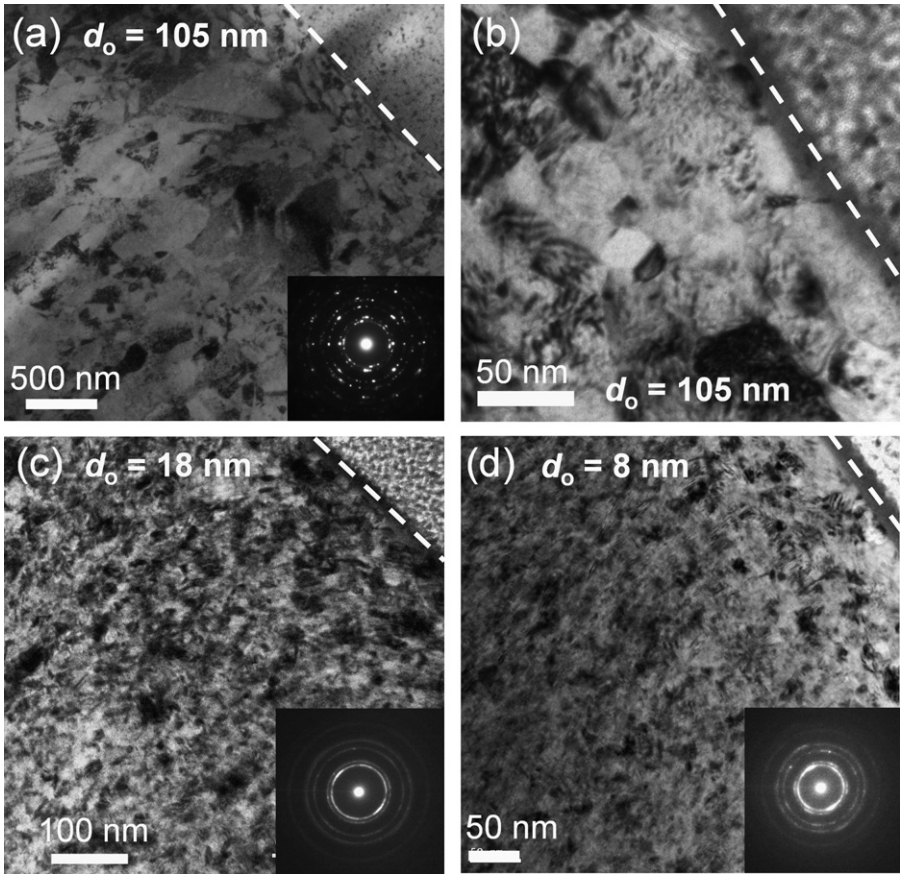

Fig. 4. TEM micrographs of the grain structure near the wear surface for (a, b) an initial grain size (d_o) of 105 nm, (c) d_o=18 nm, and (d) d_o=8 nm. The sample with d_o=105 nm exhibits slight grain refinement near the wear surface, while the smaller grain size samples experience no obvious structural evolution.

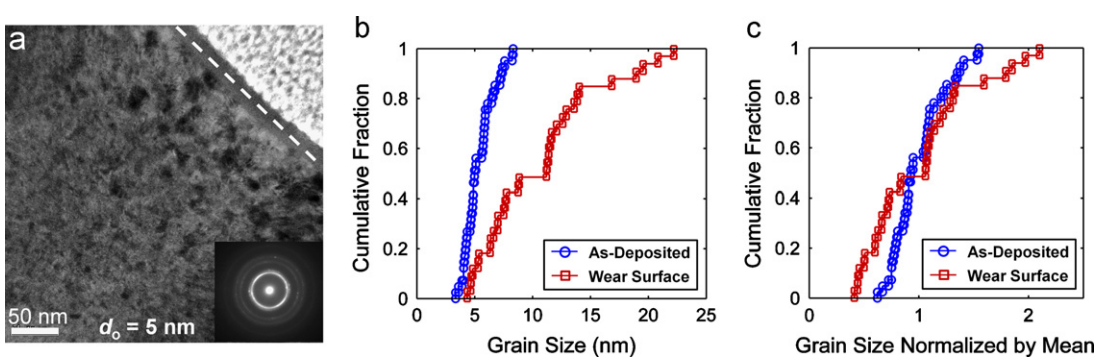

Fig. 5. (a) A bright field TEM micrograph from the d_o=5 nm sample showing structural evolution characterized by a relatively smooth transition from the bulk microstructure to a coarser near-surface grain size. Grain size measurements from the as-deposited material and the wear surface (defined as within 100 nm of the surface) are presented as (b) a cumulative distribution plot and (c) a mean-normalized cumulative distribution plot.

structural evolution in these samples. At these grain sizes, grain boundary dislocation processes dominate plasticity.

The Ni–W alloy with an as-deposited grain size of 5 nm, where the apparent deviation from Archard scaling was observed, was investigated next. A TEM micrograph taken close to the wear surface is presented in Fig. 5(a), with the surface again marked by a dashed white line. Comparison of the material near the surface with that further below provides evidence that this alloy experiences grain growth due to the wear process. A relatively smooth transition from the bulk microstructure to a coarser near-surface grain size is observed. Without a clear boundary between the bulk and wear damaged material, we choose a somewhat arbitrary cutoff depth of 100 nm here to define the material near the wear surface. Grain size measurements from the as-deposited and worn material are presented as cumulative distribution plots in Fig. 5(b). Comparison of the two curves shows that wear has increased the average grain size from 5 nm to 11 nm.

Recent studies have found evidence that applied stress can act as a driving force for grain boundary migration and grain rotation leading to grain coarsening in nanocrystalline materials [26–28]. Since only select boundaries move during mechanically-driven grain growth, such a process changes the characteristic shape of the grain size distribution, i.e., mechanically driven grain growth is "abnormal". To investigate the possibility that our observed microstructural evolution is mechanically-driven, we present mean-normalized grain size distributions in Fig. 5(c). This figure shows that the grain size distribution of the worn material has broadened and changed shape, reminiscent of other reports of

deformation-induced structural evolution [17,26]. This contrasts with what would be expected if the observed grain growth was thermally-driven by frictional heating, where one would expect the mean-normalized grain size distribution to retain its shape in Fig. 5(c).

4. Discussion

4.1. Deviation from Archard scaling

The observed grain growth alone cannot explain the fact that our $d_o = 5$ nm specimen wears less than would be expected from its as-deposited properties. For the extent of grain growth observed, one would expect hardness of the material to remain roughly constant (cf. Fig. 1), while our material behaves as though it has hardened during the wear process. This nominally unexpected result can be attributed to the fact that grain boundary relaxation, the reduction of excess interfacial defects, accompanies (and likely precedes) grain growth in nanocrystalline Ni–W [19,29]. Whereas the observed grain growth should result in no change in hardness, grain boundary relaxation is well established as contributing to hardening in both nanocrystalline Ni–W [19,30] and other alloys [31,32]. In fact, Rupert et al. [30] studied this phenomenon in detail and found that grain boundary relaxation can increase hardness by ~30% for a specimen with an average grain size (6 nm) that is similar to that of our sample in question. The similarity between the magnitudes of this relaxation hardening effect and our deviation from Archard scaling (30%) supports the hypothesis that grain boundary relaxation hardening during structural evolution is responsible for the observed wear behavior. In fact, if wear-induced grain boundary relaxation increased the hardness of the surface material by the 30% observed by Rupert et al. [30] and our present wear data were corrected (i.e., plotted against post-wear as opposed to pre-wear hardness), the wear response of the $d_o = 5$ nm sample would follow the predictions of Eq. (1). In Fig. 3(b), we show the effect of such a correction; the errant data point would fall on the dotted blue line corresponding to the Archard law if we presume a 30% hardening due to grain boundary relaxation. Unfortunately, hardness measurements are very unreliable at the extremely fine depths (~10 nm) that would be required to evaluate the structural evolution region directly, even with nanoindentation.

4.2. Abrasive versus sliding wear

Our observations here for Taber abrasion can be compared with the previous report of structural evolution during pin-on-disk sliding wear of nanocrystalline Ni–W [17]. Representative TEM micrographs of the near-surface microstructure following Taber abrasion and pin-on-disk wear tests are presented in Fig. 6 for comparison. In both cases, structural evolution is observed near the wear surface for the finest grain sizes where Archard scaling is violated. However, while pin-on-disk wear produces a thick grain growth layer sharply separated from the base material (Fig. 6(b)), Taber abrasion samples show a more gradual transition between the wear damaged and bulk microstructures (Fig. 6(a)). To understand this difference, it is important to recognize that two parameters influence the formation of an evolved layer: (1) local shear stress and (2) rate of material removal. High shear stresses promote mechanically-driven grain growth [26], while slow material removal rates will allow a distinct evolved layer to form.

To address the first point, we evaluate the maximum principal shear stress of Taber abrasion and pin-on-disk wear for the experimental conditions used here and in [17], respectively, using the Hertzian theories for cylinder-on-plate and sphere-on-plate contact [33]. Such an analysis neglects several important factors which are unknown, such as the tangential loading from frictional resistance and the roughness/asperities that develop during testing. Nonetheless, this approach allows us to make a relative comparison of the applied, global contact stress in each test. The following inputs were used: Young's moduli of Ni (207 GPa [34]), Al_2O_3 (380 GPa [35]), and WC (680 GPa [35]), Poisson's ratio of Ni (0.31 [34]), Al_2O_3 (0.24 [35]), and WC (0.24 [35]), Al_2O_3 Taber abrasion wheel diameter of 51.9 mm, and WC pin-on-disk counterbody diameter of 6 mm.

The calculated maximum principal shear stresses for each test are included above the TEM micrographs in Fig. 6, showing that the stress in the pin-on-disk experiments ($\tau_{max,Hertzian} = 460$ Mpa) is approximately 42 times larger than the stress in the Taber abrasion experiments ($\tau_{max,Hertzian} = 11$ MPa) for the testing conditions considered here. This large change is mainly due to the difference in apparent contact area for the two tests; pin-on-disk testing focuses the applied load at a small contact between a sphere and the surface while Taber abrasion spreads the contact load over a wide area where the abrasive wheel lies on the surface. Of course, local asperity contacts can be expected to induce higher local stresses, but the

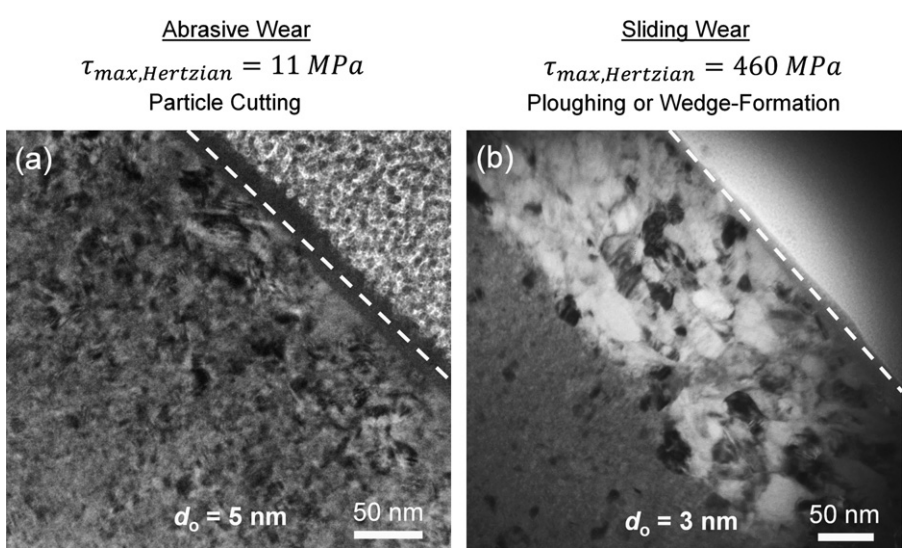

Fig. 6. TEM micrographs taken close to the wear surface for specimens tested with (a) Taber abrasion and (b) pin-on-disk sliding. The maximum principal shear stress calculated from Hertzian mechanics and the dominant abrasive mechanism expected for each experiment are shown above the micrographs.

global applied Hertzian stress in Taber testing is quite low; the testing method is sometimes referred to as "low stress abrasion" for this reason [36,37].

The rate at which material is removed from the surface is important as well, as the near-surface region must experience the contact stresses without immediate removal in order to produce a distinct grain growth layer. For abrasive contact, wear can occur by cutting, wedge-formation, or plowing mechanisms [38]. Cutting results in the fastest material removal rate, but requires particles which are oriented at large contact angles with respect to the sample surface. Taber abrasion wheels are made from ceramic particles pressed together with limited binder, with new sharp abrasive particles exposed as old particles break off the surface. The particles have a distribution of contact angles with the surface and many can be expected to have a contact angle greater than the critical value required for activation of the cutting mechanism, similar to the case for abrasive papers [39]. Unlike Taber wheels, the asperities on the pin surface in pin-on-disk experiments only arise due to plastic deformation (there is no inherent fresh supply of abrasive particles); for this reason, they tend to be blunt and unlikely to cause material removal through cutting. Therefore, wear loss during the pin-on-disk experiments occurs mainly from plowing or wedge-formation action, where there is a great deal of plastic deformation but little material removal.

When considered together, the lower stress and the faster material removal of Taber abrasion as compared to sliding wear explain why a more gradual structural evolution is observed here. Pin-on-disk sliding conditions are much more conducive to the formation of a distinct grain growth layer, as material is under high applied stresses for multiple passes before it is removed. For Taber abrasion, the fast material removal due to particle cutting will tend to shrink the evolved layer as it slowly tries to grow under the low applied contact stress. The end result is grain size gradient with coarsened grains only found very close to the surface, with hardened material being removed as it is formed. This suggests that wear-induced hardening may be of greater benefit in sliding wear than it is in abrasive wear conditions, where the transience of the hardened layer renders it less effective as a wear inhibitor.

5. Conclusions

The abrasive wear resistance of nanocrystalline Ni–W alloys with grain sizes spanning the Hall–Petch breakdown was studied using Taber abrasion testing. While our larger grain size samples (8–105 nm) show that reducing grain size into the nanocrystalline range can significantly improve wear resistance following predictions from the Archard equation, we observe considerable less wear loss than would be expected at our finest grain size of 5 nm. The wear damage process causes mechanically-driven grain growth near the surface in this sample. Specifically, a gradual transition from larger grains near the surface to smaller grains in the interior of the material is observed. Grain boundary relaxation is expected to accompany this grain growth, and can explain the magnitude of the improved wear resistance observed here. Comparison of these results with pin-on-disk wear experiments from the literature provides evidence that the level of structural evolution in nanocrystalline metals depends on the details of the wear conditions, with the lower contact stresses and increased particle cutting of Taber abrasion leading to a more subtle evolution of the near-surface structure than is observed in pin-on-disk sliding experiments. The results presented here demonstrate that the grain boundary-dominated deformation mechanisms which control plasticity at extremely fine nanocrystalline grain sizes can, in fact, improve wear performance by introducing a dynamic microstructure which outperforms as-prepared mechanical properties.

Acknowledgments

This work was supported by the US Army Research Office, under Contract W911NF-09-1-0422.

References

[1] J.F. Archard, Contact and rubbing of flat surfaces, Journal of Applied Physics 24 (1953) 981–988.
[2] A. Leyland, A. Matthews, On the significance of the H/E ratio in wear control: a nanocomposite coating approach to optimised tribological behaviour, Wear 246 (2000) 1–11.
[3] M.M. Khruschov, Principles of abrasive wear, Wear 28 (1974) 69–88.
[4] M. Shafiei, A.T. Alpas, Effect of sliding speed on friction and wear behaviour of nanocrystalline nickel tested in an argon atmosphere, Wear 265 (2008) 429–438.
[5] M. Shafiei, A.T. Alpas, Friction and wear mechanisms of nanocrystalline nickel in ambient and inert atmospheres, Metallurgical and Materials Transactions A—Physical Metallurgy and Materials Science 38A (2007) 1621–1631.
[6] Y.S. Zhang, Z. Han, K. Wang, K. Lu, Friction and wear behaviors of nanocrystalline surface layer of pure copper, Wear 260 (2006) 942–948.
[7] W.L. Li, N.R. Tao, Z. Han, K. Lu, Comparisons of dry sliding tribological behaviors between coarse-grained and nanocrystalline copper, Wear 274 (2012) 306–312.
[8] X.S. Guan, Z.F. Dong, D.Y. Li, Surface nanocrystallization by sandblasting and annealing for improved mechanical and tribological properties, Nanotechnology 16 (2005) 2963–2971.
[9] D.J. Guidry, K. Lian, J.C. Jiang, E.I. Meletis, Tribological behavior of nanocrystalline nickel, Journal of Nanoscience and Nanotechnology 9 (2009) 4156–4163.
[10] Z.N. Farhat, Y. Ding, D.O. Northwood, A.T. Alpas, Effect of grain size on friction and wear of nanocrystalline aluminum, Materials Science and Engineering A 206 (1996) 302–313.
[11] D.H. Jeong, U. Erb, K.T. Aust, G. Palumbo, The relationship between hardness and abrasive wear resistance of electrodeposited nanocrystalline Ni–P coatings, Scripta Materialia 48 (2003) 1067–1072.
[12] D.H. Jeong, F. Gonzalez, G. Palumbo, K.T. Aust, U. Erb, The effect of grain size on the wear properties of electrodeposited nanocrystalline nickel coatings, Scripta Materialia 44 (2001) 493–499.
[13] C.A. Schuh, T.G. Nieh, T. Yamasaki, Hall–Petch breakdown manifested in abrasive wear resistance of nanocrystalline nickel, Scripta Materialia 46 (2002) 735–740.
[14] K.S. Kumar, H. Van Swygenhoven, S. Suresh, Mechanical behavior of nanocrystalline metals and alloys, Acta Materialia 51 (2003) 5743–5774.
[15] J. Schiotz, T. Vegge, F.D. Di Tolla, K.W. Jacobsen, Atomic-scale simulations of the mechanical deformation of nanocrystalline metals, Physical Review B 60 (1999) 11971–11983.
[16] Z.W. Shan, E.A. Stach, J.M.K. Wiezorek, J.A. Knapp, D.M. Follstaedt, S.X. Mao, Grain boundary-mediated plasticity in nanocrystalline nickel, Science 305 (2004) 654–657.
[17] T.J. Rupert, C.A. Schuh, Sliding wear of nanocrystalline Ni–W: structural evolution and the apparent breakdown of Archard scaling, Acta Materialia 58 (2010) 4137–4148.
[18] A.J. Detor, C.A. Schuh, Tailoring and patterning the grain size of nanocrystalline alloys, Acta Materialia 55 (2007) 371–379.
[19] A.J. Detor, C.A. Schuh, Microstructural evolution during the heat treatment of nanocrystalline alloys, Journal of Materials Research 22 (2007) 3233–3248.
[20] ASTM, ASTM International, Standard B183-79, West Conshohocken, PA, 2009.
[21] L.A. Giannuzzi, F.A. Stevie, Introduction to Focused Ion Beams: Instrumentation, Theory, Techniques, and Practice, Springer, New York, NY, 2005.
[22] ASTM, ASTM International, Standard G195-08, West Conshohocken, PA, 2008.
[23] J.R. Trelewicz, C.A. Schuh, The Hall–Petch breakdown in nanocrystalline metals: a crossover to glass-like deformation, Acta Materialia 55 (2007) 5948–5958.
[24] A. Emge, S. Karthikeyan, D.A. Rigney, The effects of sliding velocity and sliding time on nanocrystalline tribolayer development and properties in copper, Wear 267 (2009) 562–567.
[25] J.B. Singh, J.G. Wen, P. Bellon, Nanoscale characterization of the transfer layer formed during dry sliding of Cu–15 wt% Ni–8 wt% Sn bronze alloy, Acta Materialia 56 (2008) 3053–3064.
[26] T.J. Rupert, D.S. Gianola, Y. Gan, K.J. Hemker, Experimental observations of stress-driven grain boundary migration, Science 326 (2009) 1686–1690.
[27] J.W. Cahn, Y. Mishin, A. Suzuki, Coupling grain boundary motion to shear deformation, Acta Materialia 54 (2006) 4953–4975.
[28] M. Legros, D.S. Gianola, K.J. Hemker, In situ TEM observations of fast grain-boundary motion in stressed nanocrystalline aluminum films, Acta Materialia 56 (2008) 3380–3393.
[29] N.Q. Vo, R.S. Averback, P. Bellon, A. Caro, Limits of hardness at the nanoscale: molecular dynamics simulations, Physical Review B 78 (2008) 4.
[30] T.J. Rupert, J.R. Trelewicz, C.A. Schuh, Grain boundary relaxation strengthening of nanocrystalline Ni–W alloys, Journal of Materials Research 27 (2012) 1285–1294.

[31] T. Volpp, E. Goring, W.M. Kuschke, E. Arzt, Grain size determination and limits to Hall–Petch behavior in nanocrystalline NiAl powders, Nanostructured Materials 8 (1997) 855–865.
[32] J.R. Weertman, Hall–Petch strengthening in nanocrystalline metals, Materials Science and Engineering A 166 (1993) 161–167.
[33] K.L. Johnson, Contact Mechanics, Cambridge University Press, Cambridge; New York, 1985.
[34] Metals Handbook, Properties and Selection: Nonferrous Alloys and Pure Metals, American Society for Metals, Metals Park, OH, 1989, vol. 2.
[35] J.F. Shackleford, W. Alexander, J.S. Park, CRC Materials Science and Engineering Handbook, 2nd ed., CRC Press, Boca Raton, FL, 1994.
[36] D.M. Kennedy, M.S.J. Hashmi, Methods of wear testing for advanced surface coatings and bulk materials, Journal of Materials Processing Technology 77 (1998) 246–253.
[37] K. Holmberg, A. Matthews, Coatings Tribology: Properties, Mechanisms, Techniques and Applications in Surface Engineering, Elsevier Science, Amsterdam; Boston; London, 2009.
[38] K. Hokkirigawa, K. Kato, An experimental and theoretical investigation of plowing, cutting and wedge formation during abrasive wear, Tribology International 21 (1988) 51–57.
[39] T.O. Mulhearn, L.E. Samuels, The abrasion of metals: a model of the process, Wear 5 (1962) 478–498.